Quasi real-time Raman studies on the growth of Cu–In–S thin films

Eveline Rudigier[a)]
Hahn-Meitner Institut, Division Solar Energy, Glienicker Strasse 100, 14109 Berlin, Germany

Beatriz Barcones
Departament d'Electrònica, Enginyeria i Materials Electrònics (EME), Universitat de Barcelona, Martí i Franquès 1, 08028 Barcelona, Spain

Ilka Luck
Hahn-Meitner Institut, Division Solar Energy, Glienicker Strasse 100, 14109 Berlin, Germany

T. Jawhari-Colin
Laboratori Raman, Serveis Cientificio-Tècnics, Universitat de Barcelona, Martí i Franquès 1, 08028 Barcelona, Spain

Alejandro Pérez-Rodríguez
Department d'Electrònica, Enginyeria i Materials Electrònics (EME), Universitat de Barcelona, Martí i Franquès 1, 08028 Barcelona, Spain

Roland Scheer
Hahn-Meitner Institut, Division Solar Energy, Glienicker Strasse 100, 14109 Berlin, Germany

(Received 15 July 2003; accepted 14 January 2004)

In this work annealing and growth of $CuInS_2$ thin films is investigated with quasireal-time *in situ* Raman spectroscopy. During the annealing a shift of the Raman A_1 mode towards lower wave numbers with increasing temperature is observed. A linear temperature dependence of the phonon branch of $-2\ cm^{-1}/100\ K$ is evaluated. The investigation of the growth process (sulfurization of metallic precursors) with high surface sensitivity reveals the occurrence of phases which are not detected with bulk sensitive methods. This allows a detailed insight in the formation of the $CuInS_2$ phases. Independent from stoichiometry and doping of the starting precursors the CuAu ordering of $CuInS_2$ initially forms as the dominating ordering. The transformation of the CuAu ordering into the chalcopyrite one is, in contrast, strongly dependent on the precursor composition and requires high temperatures. © *2004 American Institute of Physics.* [DOI: 10.1063/1.1667009]

I. INTRODUCTION

Chalcopyrite semiconductor materials have been well established as absorber layers in high efficient solar cell devices.[1] Among these, $CuInS_2$ (CIS) is promising because of its bandgap being well suited to the solar spectrum. As the understanding of this material is far from being complete structural characterization is needed. Real-time x-ray diffraction (XRD) experiments have already been performed during the growth of the $CuInS_2$ films[2] which gave an insight into processes in the bulk. But an additional method clarifying the reactions taking place near the surface is as well desirable. Therefore, studies of the vibrational properties via *in situ* Raman spectroscopy appear promising.

One advantage of Raman spectroscopy is that the different orderings of CIS, such as the chalcopyrite (CH) and the CuAu (CA) ordering are observable.[3] Furthermore, Raman spectroscopy is a contactless method which can be used for quality assessment.[4] Previously it has been found that the presence of CuAu ordering in the $CuInS_2$ films gives rise to a deterioration of the solar cell performance.[5] The presence of this ordering in the completed $CuInS_2$ layers, however, is dependent on the starting precursor composition.[6] Therefore, it is important to investigate the growth of CIS in detail.

It is known that different Cu/In ratios in chalcopyrite films as well as the presence of doping elements have an influence on the structural and electronic properties.[7,8] A dopant of primarily importance for chalcopyrite thin films in general is the element Na.[9] The role of Na, in particular for the growth process, is currently not understood.

In this study, we first performed annealing experiments of completed $CuInS_2$ layers with different compositions and determined the temperature dependence of the main phonon mode of CIS. In a second step, sulfurization experiments of Cu–In precursors have been investigated by quasireal-time Raman measurements. We show that the CIS formation starts with the CuAu ordering being the dominant one independent from the precursor composition. We are also able to follow the transformation of the CuAu ordering into chalcopyrite ordering which is dependent on the precursor starting composition.

II. EXPERIMENT

For the presented *in situ* Raman experiments a portable vacuum chamber has been constructed. A base pressure of about 1×10^{-6} mbar is provided. Heating of the substrates up to 500–550 °C results from thermal radiation of a graphite heater, while cooling down takes place without any tem-

a)Author to whom correspondence should be addressed; electronic mail: rudigier@hmi.de

perature regulation. For the temperature measurement a thermocouple is situated between the backside of the substrate and the heater. A Knudsen source provides sulfur vapor from elemental sulfur. The working temperature for the sulfur source is at 190 °C providing a sulfur partial pressure of around 1×10^{-4} mbar. The chamber is equipped with an especially designed optical window for excitation and detection of the Raman signal. A T64000 Jobin Yvon Raman setup has been used with an excitation line of 514.5 nm from an Ar^+ laser. For this wavelength we calculated a penetration length of 150 nm in $CuInS_2$.[10] The Raman spectra were taken with a time resolution of 30 or 60 s. Fitting of the Raman lines was performed using single or multiple Lorentzians.

In situ Raman experiments were performed during sulfurization of metal precursors (growth experiments) and during annealing (annealing experiments) of presulfurized Cu–In–S layers. For the latter the Cu-rich presulfurized Cu–In–S layers had been previously etched in KCN to result in the stoichiometric composition. No additional sulfur was supplied during the annealing experiments. The formation of the precursors was accomplished by sequential dc magneton sputtering of Mo/Cu/In on soda–lime glass as described elsewhere.[11] A NaF layer was introduced between Mo and Cu for some samples by evaporation. Different copper-to-indium molar ratios (Cu-poor: 0.8, Cu-rich: 1.8) have been used, resulting in a final $CuInS_2$ film thickness of 2 μm. For the annealing experiments the following temperature profile has been realized: heating up period of 30 min from room temperature up to 500 °C, followed by a holding period at this temperature of 10 min. For the growth experiments a 20 min ramp up to 550 °C was used, followed as well by a holding period of 10 min at top temperature.

III. RESULTS

In Fig. 1, a survey of Raman spectra from samples during different processing steps is presented. In the spectral range of 300 cm^{-1} we find two distinct peaks at around 290 and 305 cm^{-1} which can be assigned to the A_1 modes of the chalcopyrite and CuAu ordering, respectively.[12,13] If this spectral range is fitted by a single line, different peak positions would be obtained depending on the prevailing ordering. Accordingly, an intermediate peak position indicates the two orderings occurring in one sample. Certainly, the shape of the peak is also affected by the presence of these two contributions. In some cases it is even possible to detect both peaks well separated, as shown in spectrum (b) of Fig. 1. In addition, peaks at 260, 340, and 470 cm^{-1} can be discerned for different growth experiments which we assign to the phases, CuS, $CuIn_5S_8$, and CuS, respectively. Some spectra also show a very weak contribution around 140 cm^{-1} [see Fig. 1(e)], which can be attributed to vibrational modes from the β-In_2S_3 phase.

Figure 2 presents the Raman peak positions of the $CuInS_2$ A_1 modes for the annealing experiments as a function of the substrate temperature. The peak positions are obtained from a single Lorentzian fit. The investigated samples are: (1) Cu rich (Cu/In=1.8), (2) Cu poor (Cu/In=0.8) with Na, and (3) Cu poor (Cu/In=0.8) without Na. The data are shown for the complete annealing process where the heating and cooling periods are indicated by arrows. All samples show a shift towards smaller wave numbers with increasing temperature. A linear correlation is most obvious for the Cu-rich sample, while the data of the Cu-poor samples appear

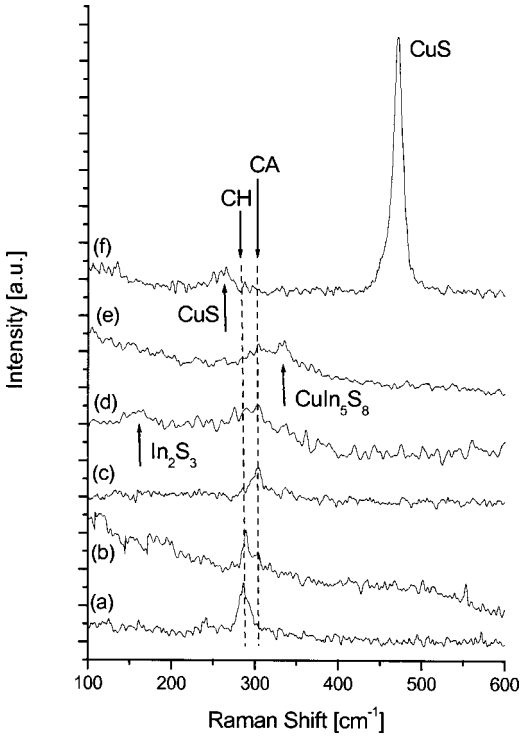

FIG. 1. Raman scattering intensities vs wave numbers for the annealing experiments (a) Cu-rich (Cu/In=1.8) sample, (b) Cu-poor (Cu/In=0.8) sample with sodium, and (c) Cu-poor (Cu/In=0.8) sample without sodium. Raman spectra for growth experiments: (d) Cu-poor sample without sodium in the heating up period, (e) Cu-poor sample without sodium in the cooling down period, and (f) Cu-rich sample in the cooling down period.

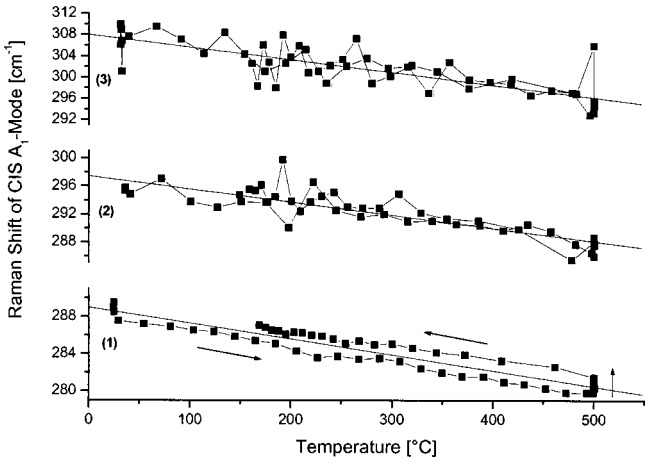

FIG. 2. The spectral peak shift of the CIS main mode is presented as a function of the temperature for the annealing experiments of samples with a: (1) Cu-rich (Cu/In=1.8), (2) Cu-poor (Cu/In=0.8) with sodium, and (3) Cu-poor (Cu/In=0.8) without sodium composition. The Cu-rich sample has prior been etched. The markers show the experimentally determined data, while the dashed line gives the fit results of this temperature effect. The process sequence is indicated by arrows.

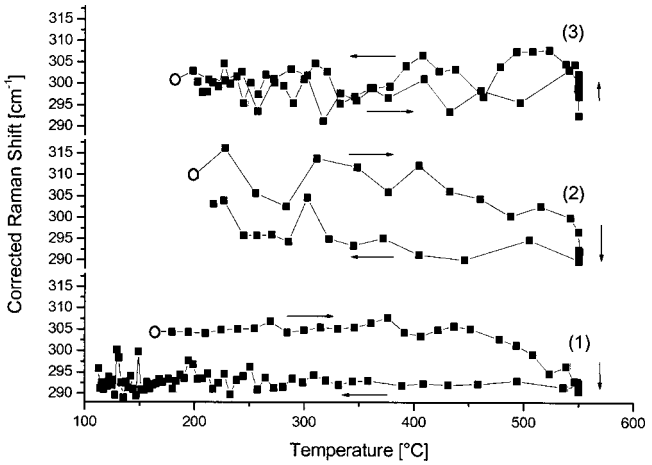

FIG. 3. The Growth experiments for samples: (1) Cu rich (Cu/In=1.8), (2) Cu poor (Cu/In=0.8) with Na, and (3) Cu poor (Cu/In=0.8) without Na are presented as the peak shift of the CIS main mode vs the temperature. The CIS main mode obtained from a single Lorentzian fit is given as a function of the substrate temperature. The peak shift is corrected by the temperature dependence of the annealing experiments. The arrows indicate the process sequence and the round markers the beginning of the CIS formation.

with more noise. Remarkably, the CIS peak positions differ: starting from sample 1 (Cu rich) with the lowest Raman shift (289 cm^{-1}), continuing with the Cu-poor sample 2 with sodium (297 cm^{-1}), up to sample 3 (Cu poor without Na) at around 308 cm^{-1}. A fit of the data as depicted in Fig. 2 yields for the Cu-rich sample a temperature gradient of

$$\frac{\partial(\Delta\tilde{\nu})}{\partial T} \approx -\frac{1.7\ \mathrm{cm}^{-1}}{100\ \mathrm{K}}.$$

We compared the peak position at room temperature with the peak position at top temperature and calculated a relative thermal change in the vibrational frequency of $\approx 6.3 \times 10^{-5}\,K^{-1}$. For the Cu-poor sample with sodium the relative temperature gradient is slightly higher ($\approx$1.9 cm^{-1}/100 K), while the Cu-poor sample without any doping shows a significant higher value of approximately 2.3 cm^{-1}/100 K. The variance of the peak positions as well as of the temperature gradients indicate the presence of a second phase besides the CH ordering for the Cu-poor prepared samples. For the Cu-rich experiment at top temperature a small shift towards higher wave numbers has been observed, which remains present in the cooling-down period. This may be due to a small temperature difference between the substrate and the thermocouple. A different explanation could be a real change in the lattice parameter. The temperature gradients and peak positions from the annealing experiments in the following are useful to correct the data obtained from the growth experiments. Not considered here is the increase in intensity of the Raman modes with increasing temperature. This increase is to be expected according to the Bose–Einstein statistic of phonons.

Figure 3 shows the CIS peak positions versus the process temperature for the sulfurization of the precursors [Cu rich (Cu/In=1.8) (1), Cu poor (Cu/In=0.8) with Na (2), Cu poor (Cu/In=0.8) without Na (3)]. The temperature of the initial formation of CIS can be judged from the first appearance of the A_1 mode. The course of the growth process is indicated by the arrows. Hereby, the peak positions have been corrected by the linear temperature dependence of the corresponding annealing experiments from Fig. 2. Having substracted the temperature dependence, constant peak positions are to be expected. For the Cu-rich experiment CIS formation starts with high wave numbers (around 305 cm^{-1}) at approximately 165 °C. Increase of the temperature above $\approx$380 °C induces a decrease of the A_1 mode position (down to around 292 cm^{-1}). During the holding and cooling down period no further significant change has been observed. For sample 2 (Cu poor with Na), a similar behavior is found: starting from 200 °C up to 400 °C almost constant values around 310 cm^{-1} for the CIS main Raman mode are observed, while for temperatures >400 °C a decline down to around 295 cm^{-1} occurs; during the remaining holding period and cooling down period the A_1 mode does not shift significantly. For the Cu-poor experiment without Na the position of the A_1 mode starting from its first appearance of around 180 °C remains at 308 cm^{-1} for both the heating and the cooling periods. The initial formation of CIS is detected at higher temperatures for the two Cu-poor samples, especially the sample containing Na.

Figures 4(a) and 4(b) give the areal intensity of several Raman lines as a function of the process time for a Cu-rich and a Cu-poor sulfurization, respectively. Here, the CIS signals are on the one hand fitted using a single Lorentzian and on the other hand split up into CH and CA ordering using two Lorentzians. For reference purposes, the substrate temperature profile is plotted in the header of these figures. In the heating up period of the Cu-rich experiment [Fig. 4(a)] the 470 cm^{-1} line of CuS is detected at around 150 °C. At a slightly higher temperature (165 °C) signals belonging to CIS are found, while simultaneously the CuS phase vanishes. Up to 500 °C the CA ordering is highly dominating the CIS signal. Further increase of the temperature is accompanied by a decreasing CA signal until it vanishes as soon as the top temperature is reached. The peak belonging to the CH ordering can be observed for the whole remaining process, with a maximum in intensity at 550 °C. In the cooling down period again peaks of the CuS phase appear (at around 180 °C). The data in Fig. 4(b) are given for a growth experiment of a Cu-poor precursor with no additional sodium. Here, the first observed phase in the heating up period is CuS (around 165–210 °C). Initial CIS formation takes place at 180 °C. Between 270 and 350 °C a weak peak at 140 cm^{-1} is found, which we assign to β-In_2S_3 [cf. sample (d) in Fig. 1]. Signals of both the CH and CA ordering can be found down to 200 °C in the cooling period. The CA ordering appears to be dominant. With the vanishing CIS signals the appearance of the In-rich phase $CuIn_5S_8$ is indicated by the broad signal at around 340 cm^{-1} [cf. Fig. 1(e)]. This phase remains as the only detectable one until the end of the process.

In principal the growth process of the Cu-poor sample with sodium is similar to the one of the Cu-poor sample without sodium. The main difference is that at the end of the process β-In_2S_3 instead of the $CuIn_5S_8$ phase occurs near the surface.

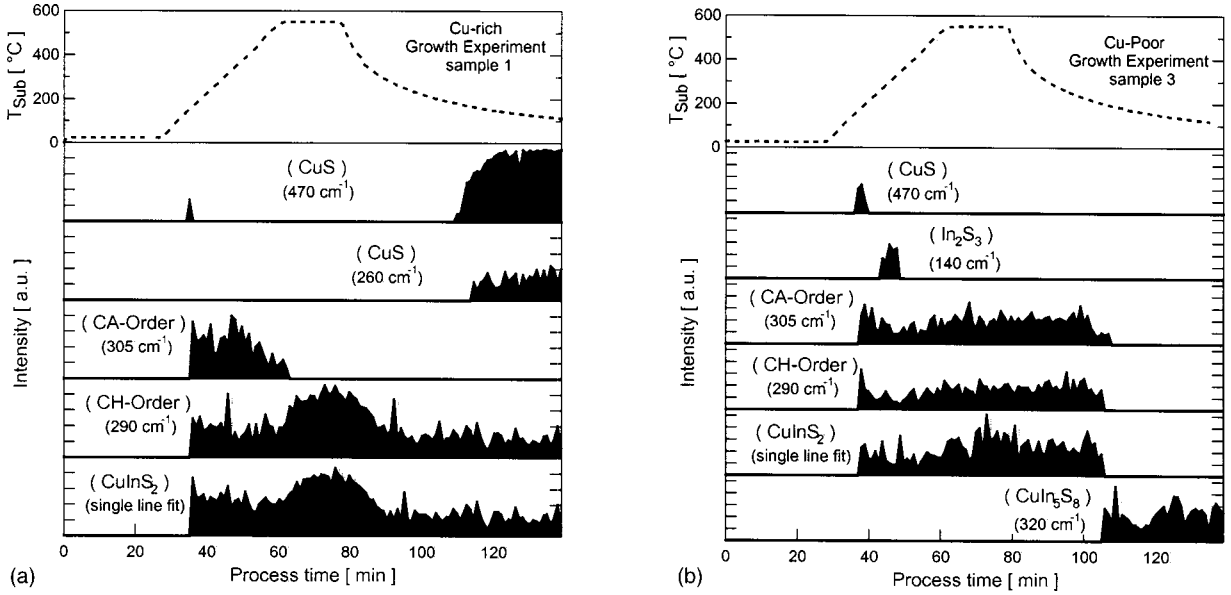

FIG. 4. (a) Temperature profile and areal intensity of characteristic Raman modes for the sulfurization process of Cu-rich (Cu/In=1.8) prepared samples vs process time. (b) Temperature profile and areal intensity of characteristic Raman modes for the sulfurization process of Cu-poor (Cu/In=0.8) prepared samples without sodium vs process time.

IV. DISCUSSION

The annealed samples differ in their absolute peak position of the A_1 mode if this mode is fitted by a single line. The value for the Cu-rich sample (289 cm^{-1}) fits with the theoretical value for the A_1 mode of the CH ordering (294 cm^{-1}), and even better agreement is found with experimentally determined values (290 cm^{-1}) from other groups.[13,14] For the Cu-poor $CuInS_2$ layer without Na the experimental value of 308 cm^{-1} is in good agreement with the position of the A_1 mode for the CA ordering of 305 cm^{-1}. This difference between Cu-rich and Cu-poor films has already been reported for coevaporated films.[15] The determined peak position for the Cu-poor sample with Na lies between the values of CH and CA. Obviously, in this case the two orderings of CIS coexist with a slightly higher share of the chalcopyrite ordering. Therefore, we conclude that doping of $CuInS_2$ with sodium increases the amount of the CH ordering in Cu-poor films.

The annealing experiments show that an increase of temperature is combined with a shift of the peak position towards smaller wave numbers. In general the amplitudes of the lattice vibrations increase with temperature and the influence of the potential modified by the anharmonicity of the lattice on the atoms is becoming stronger. In the Grüneisen approach the relative change in the phonon frequency, $\delta(\Delta\tilde{\nu}_{\mathbf{q},j})/\tilde{\nu}_{\mathbf{q},j}$, is assumed to be proportional to the relative change of the volume $(\delta(\Delta\tilde{\nu}_{\mathbf{q},j})/\tilde{\nu}_{\mathbf{q},j}=-\gamma(\delta V/V))$. This expression, where γ describes the Grüneisen parameter, is independent from the absolute phonon frequency and the type of the mode. It follows that the thermal expansion coefficient α can be expressed as

$$\alpha=\frac{\gamma\kappa C_V}{3V},$$

with κ the compressibility, C_V the specific heat capacity, and V the volume. With the definitions for κ and C_V and the above expression for α, the temperature dependence of the phonon frequency is approximately characterized by

$$\frac{\partial(\Delta\tilde{\nu})}{\partial T}=\left(\frac{\partial(\Delta\tilde{\nu})}{\partial V}\right)\left(\frac{\partial V}{\partial T}\right)=\left(\frac{\partial(\Delta\tilde{\nu})}{\partial V}\right)\left(\frac{\partial V}{\partial p}\right)\left(\frac{\partial p}{\partial T}\right)$$
$$=-3\gamma\alpha\nu.$$

Thus, a decrease of frequency with temperature will occur. For most solids such behavior has been experimentally observed. The above equation yields a temperature dependence of the frequency shift for the A_1 mode of CIS of

$$\frac{\partial(\Delta\tilde{\nu})}{\partial T}=-\frac{1.13\ \mathrm{cm}^{-1}}{100\ \mathrm{K}}.$$

Here, the thermal linear expansion coefficient for CIS (CH ordering) in the temperature range $T=200-600\,^{\circ}\mathrm{C}$ of $\alpha=1.0\times10^{-5}\,\mathrm{K}^{-1}$,[16] and the Grüneisen parameter for $CuInSe_2$ ($\gamma=1.3$)[17] have been used. The latter has been chosen because of a lack of data for CIS in the literature. As the thermal expansion coefficients for $CuInS_2$ and $CuInSe_2$ are nearly identical, the Grüneisen parameter supposedly has a similar value. The so determined frequency shift is an approximation, because for the calculation no differences between the phonon branches have been considered. Furthermore, only the first term of the Taylor expansion for the peak shift with temperature has been taken into account. Terms with a higher order of the Taylor series describe phonon decay and four-phonon processes. Despite all these simplifications, a fair agreement between the theoretical and experimental temperature coefficient has been found for the CH ordering of the Cu-rich sample. Higher values of $\partial(\Delta\tilde{\nu})/\partial T$ for the Cu-poor experiments (with and without Na) are due to the coexisting CA ordering. It is likely that the phonon

frequencies of this phase show a different temperature dependence. Therefore, for the Cu-poor samples containing Na the experimental $\partial(\Delta\tilde{\nu})/\partial T$ can be interpreted as a mixture of the two orderings. Supposedly, for the Cu-poor sample without Na the behavior is dominated by the CA ordering. Because of the relatively small expansion coefficient in the investigated temperature range it is valid to assume the frequency shift to be proportional to the temperature. This is indeed observed in the experiments.

In situ XRD measurements have previously been performed on the sulfurization of Cu-rich and Cu-poor precursor films.[18] For both types of precursors the starting metallic phases are $CuIn_2$ and Cu.[19] At around 140 °C $CuIn_2$ transforms into $Cu_{11}In_9$ under the release of liquid In. From the intermetallic $Cu_{11}In_9$ phase and from elemental sulfur CIS forms at approximately 200 °C in the heating period. In the Cu-rich experiment the In can react completely with the abundant elemental Cu. But due to the excess of Cu in this experiment a CuS phase appears in the cooling down period.

For the Cu-poor experiment an additional In–S compound was found as an intermediate phase. This phase may have formed from the liquid In released by the $CuIn_2 \rightarrow Cu_{11}In_9$ transformation. The further reaction to $CuInS_2$ consumes all elemental Cu now leaving no abundant Cu for the In to react. Thus In is sulfurized and is accommodated by the spinel phase $CuIn_5S_8$. The latter is only observed in Cu-poor films. Apparently, this spinel phase segregates during the cooling down period completely covering the two CIS orderings. From the XRD studies we know that CIS exists until the end, i.e., no complete transformation into this In-rich compound took place, and the assumption of $CuIn_5S_8$ as a surface coverage seems to be likely.[20]

In contrast to the Raman data presented here no CuS phase has been observed with XRD during the heating up period. Therefore, it is likely that CuS forms near the surface with a relatively small volume percentage and can only be detected by Raman. From XRD sulfurization experiments of pure Cu layers it is known that the hexagonal CuS transforms into the cubic Cu_2S.[14] However this phase appears to have a too low Raman scattering cross section as it is not observed in our experiments. Based on the phase diagram[21] the transformation $CuS \rightarrow Cu_2S$ should appear at approximately 507 °C. But as indicated by the vanishing of the CuS phase, it is likely that here the transformation occurs at a lower temperature ($\approx$200 °C). For thin films such a reaction has already been observed to take place at lower temperatures,[22] and to be dependent on the sulfur partial pressure.[23]

All growth experiments have in common that the CIS formation starts with the CA ordering being highly dominant, which partially transforms into CH. As the CIS formation proceeds at the very surface, i.e., the growth front is in the direction of the surface normal,[24] it may be argued that initially formed CA ordering at the end of the growth is covered by newly grown CH ordering, i.e., no transformation took place. But from Raman depth dependent experiments of finished layers it is known that for the Cu-rich case no CA ordering is left at all.[13] Therefore, we interpret the data in the sense of a phase transformation.

For the Cu-rich experiment the transformation CA→CH starts at around 380 °C and is completed with reaching the top temperature. The Cu-poor experiment with Na also shows the CA→CH transformation. But as can be seen at the peak position (297 cm^{-1}) here the transformation takes place only partially. For the remaining process CH and CA ordering coexist. No such transformation (CA→CH) has been observed for the Cu-poor experiment without any sodium. Here, the CIS signals are clearly dominated by the CA ordering over the whole process.

Two questions arise: First, why is the CA ordering preferred to form at first as the dominating CIS ordering independent from the precursor composition. Second, which mechanism induces the transformation into CH.

The first point might be related to the temperature. The difference in formation energy between CH and CA ordering for $CuInS_2$ has been calculated to be small (−7.8 meV/four atom).[25] The results presented here show, however, that the metastable CA ordering is energetically favored to form at low temperatures, while the CH formation requires higher energies. This has been found as well for coevaporated samples.[15] For III–V semiconductor alloys it has been theoretically shown that CuPt ordering occurs due to surface reconstructions.[26] The formation of the CA ordering may be promoted by similar effects.

In order to clarify the second question, we compare the different stoichiometries (Cu rich: Cu/In=1.8 and Cu poor: Cu/In=0.8). As soon as the temperature is high enough, the CH formation takes place as well as a recrystallization of the CA ordering. But for the recrystallization the presence of a Cu–S binary seems to be promotive: while the Cu-rich film undergoes the CA→CH transformation, no transformation here is observed for the undoped Cu-poor film. The preferred CH ordering in the presence of a Cu–S binary has also been shown for samples prepared via coevaporation. Therefore, a model has been developed, explaining the transformation by the solubility of the CA ordering in Cu_2S at a certain temperature promoting the formation of the stable CH ordering.[27]

The influence of sodium on the growth of chalcopyrites is still discussed.[9,28,29] But, as Na has a similar electronic configuration to copper, it appears possible that Na partially takes on the function of Cu. For instance, Na might imitate a Cu-rich environment by filling Cu vacancies or might form Na_2S initiating the CA→CH transformation. However, with the top temperature chosen the transformation is not complete. So far conceivable possibilities for the completion of the transformation might be on the one hand higher temperatures or on the other hand an increased amount of sodium. Further experiments have to detail this point. Another effect of sodium is that both the beginning of the formation of the CuAu phase and of the transformation into the chalcopyrite require higher temperatures. This is in accordance with results obtained from calorimetric experiments on the selenide system.[30]

V. CONCLUSIONS

We introduced Raman spectroscopy as a method for quasireal-time experiments on the chalcogenization of Cu–In

layers. Annealing experiments show a shift towards lower wave numbers of the CIS main mode with increasing temperature. The temperature dependence of the peak shift has been calculated and an approximative agreement with the experimental value has been found. The growth experiments showed that the start of growth of CIS is dominated by the CA ordering. The CH formation takes place at elevated temperature and is promoted by the presence of Cu excess or additionally supplied sodium.

ACKNOWLEDGMENTS

The authors wish to thank J. Klaer and E. Müller for their help in sample preparation. For Raman measurements the assistance of J. Alvarez is gratefully acknowledged. Part of this work has been funded by the BMBF (Contract No. 01SF0022).

[1] M. Ch. Lux-Steiner *et al.*, Thin Solid Films **533**, 361 (2000).
[2] C. Pietzker, E. Rudigier, D. Bräunig, and R. Scheer, Proceedings of 17th European Photovoltaic Solar Energy Conference, Munich, Germany, edited by B. McNelis, W. Palz, H. A. Ossenbrink, and P. Helm, 2001, Vol. 2, p. 1031.
[3] J. Alvarez-Garcia, A. Pérez-Rodríguez, B. Barcones, A. Romano-Rodríguez, J. R. Morante, A. Janotti, S.-H. Wei, and R. Scheer, Appl. Phys. Lett. **80**, 562 (2002).
[4] E. Rudigier, I. Luck, and R. Scheer, Appl. Phys. Lett. **82**, 4370 (2003).
[5] J. Alvarez-García, E. Rudigier, N. Rega, B. Barcones, R. Scheer, A. Pérez-Rodríguez, A. Romano-Rodríguez, and J. R. Morante, Thin Solid Films **431–432**, 122 (2003).
[6] J. Alvarez-Garcia, A. Perez-Rodriguez, A. Romano-Rodríguez, and J. R. Morante, J. Vac. Sci. Technol. A **19**, 232 (2001).
[7] J. Klaer, J. Bruns, R. Henniger, K. Siemer, R. Klenk, K. Ellmer, and D. Bräunig, Semicond. Sci. Technol. **13**, 1456 (1998).
[8] I. Luck, J. Kneisel, K. Siemer, J. Bruns, R. Scheer, R. Klenk, N. Janke, and D. Bräunig, Sol. Energy Mater. Sol. Cells **67**, 151 (2001).
[9] T. Tanaka, T. Yamaguchi, and A. Yoshida, Proceedings of the 11th International Conference on Ternary and Multinary Compounds, Salford, UK, edited by R. D. Tomlinson, A. E. Hill, and R. D. Pilkington, 1998, p. 329.
[10] M. Saad, S. Bleyhl, T. Ohashi, Y. Hashimoto, K. Ito, B. Mertesacker, A. Jäger-Waldau, W. Woletz, and M. C. Lux-Steiner, Proceedings 2nd World Conference on Photovoltaic Solar Energy Conversion 1, edited by J. Schmid, H. A. Ossenbrink, P. Helm, H. Ehmann, and E. D. Dunlop, 1998, Vol. 1, p. 1149.
[11] J. Klaer, J. Bruns, R. Henniger, M. Weber, R. Klenk, K. Ellmer, R. Scheer, and D. Bräunig, Proceedings of the 14th European Photovoltaic Solar Energy Conference and Exhibition, Barcelona, Spain, edited by H. A. Ossenbrink, O. Helm, and H. Ehmann, 1997, Vol. 1, p. 1307.
[12] W. H. Koschel and M. Bettini, Phys. Status Solidi B **72**, 729 (1975).
[13] J. Alvarez-Garcia, PhD thesis, University of Barcelona, Barcelona, Spain, 2002.
[14] T. Riedle, PhD thesis, Hahn-Meitner Institut Berlin, Germany, 2002.
[15] J. Alvarez-Garcia, J. Marcos-Ruzafa, A. Pérez-Rodríguez, A. Romano-Rodríguez, J. R. Morante, and R. Scheer, Thin Solid Films **361–362**, 208 (2001).
[16] C. Pietzker, PhD thesis, Hahn-Meitner Institut Berlin, Germany, 2003.
[17] H. Tanino, T. Maeda, H. Fujikake, H. Nakanishi, S. Endo, and T. Irie, Phys. Rev. B **45**, 13323 (1992).
[18] C. Pietzker, E. Rudigier, J. Klaer, I. Luck, and R. Scheer, HasyLab Annual Report, 2001, Vol. 1.
[19] W. Keppner, T. Klas, W. Körner, R. Wesch, and G. Schatz, Phys. Rev. Lett. **54**, 2371 (1985).
[20] E. Rudigier *et al.*, Thin Solid Films **431–432**, 110 (2003).
[21] D. J. Chakrabarti and D. E. Laughlin, Bull. Alloy Phase Diagrams **4**, 254 (1983).
[22] M. T. S. Nair, L. Guerrero, and P. K. Nair, Semicond. Sci. Technol. **13**, 1164 (1998).
[23] P. B. Barton, Jr., Econ. Geol. **68**, 455 (1973).
[24] K. Siemer, J. Klaer, I. Luck, J. Alvarez-Garcia, A. Pérez-Rodríguez, A. Romano-Rodríguez, and D. Bräunig, Proceedings of the 16th European Photovoltaic Solar Energy Conference, Glasgow, U.K., edited by H. Scheer, B. McNelis, W. Palz, H. A. Ossenbrink, and P. Helm, 2000, Vol. 1, p. 895.
[25] S.-H. Wei, S. B. Zhang, and A. Zunger, Phys. Rev. B **59**, R2478 (1999).
[26] S. Froyen and A. Zunger, Phys. Rev. B **53**, 4570 (1996).
[27] A. Neisser, PhD thesis, Hahn-Meitner Institut Berlin, Berlin, Germany, 2001.
[28] K. Fukuzaki, S. Kohiki, H. Yoshikawa, S. Fukushima, T. Watanabe, and I. Kojima, Appl. Phys. Lett. **73**, 1385 (1998).
[29] B. J. Stanberry, S. Kincal, S. Kim, T. J. Anderson, O. D. Crisalle, and S. P. Ahrenkiel, Proceedings of the 28th IEEE Photovoltaic Specialists Conference, Anchorage, AK, 2000, p. 440.
[30] D. Wolf and G. Müller, Jpn. J. Appl. Phys., Part 1 **39**, 173 (2000).